First-principles study of magnetism at grain boundaries in iron and nickel

Miroslav Čák,[1,2,3] Mojmír Šob,[1,2] and Jürgen Hafner[4]
[1]*Department of Chemistry, Faculty of Science, Masaryk University, CZ-611 37 Brno, Czech Republic*
[2]*Institute of Physics of Materials of the Academy of Sciences of the Czech Republic, v.v.i., CZ-616 62 Brno, Czech Republic*
[3]*Institute of Physical Engineering, Faculty of Mechanical Engineering, Brno University of Technology, CZ-616 69 Brno, Czech Republic*
[4]*Faculty of Physics and Center for Computational Materials Science, University of Vienna, A-1090 Vienna, Austria*
(Received 24 July 2007; revised manuscript received 13 June 2008; published 14 August 2008)

The geometric and magnetic structures of fully relaxed symmetrical tilt $\Sigma5(310)$ grain boundaries (GBs) in iron and $\Sigma5(210)$ GBs in nickel have been investigated using density-functional theory. We found for both GBs an enhancement of the local magnetic moments of atoms in the GB plane (2.55 μ_B for iron and 0.67 μ_B for nickel) which is correlated with the larger local atomic volume compared to the bulk. At larger distances from the GB the variation of the local magnetic moments follows the changes in the exchange splitting in the spin-polarized local density of states imposed by the local variations in the atomic geometry. When Si and Sn impurity atoms in interstitial or substitutional positions appear at the $\Sigma5(310)$ GB in iron, the local magnetic moments of iron atoms are reduced for silicon and almost unchanged for tin. We also calculated the segregation enthalpies of both impurities and confirmed the experimental fact that silicon is a substitutional and tin an interstitial segregant; the calculated values of segregation enthalpy are in good agreement with experiment.

DOI: 10.1103/PhysRevB.78.054418 PACS number(s): 61.72.Mm, 68.35.−p, 71.15.Nc, 75.70.−i

I. INTRODUCTION

Grain boundaries (GBs) represent planar defects in a homogeneous material and belong to the most important and most studied material imperfections. This is not only due to their pronounced influence on many material properties; they are also interesting from a fundamental point of view. One can look at a GB as an interface where two surfaces touch. However, the magnetism of extended defects in materials, especially of GBs, is nearly untouched problem. GBs and their properties have been the subject of numerous theoretical investigations, but very often magnetism was not included in calculations of GBs in iron and nickel.[1–5]

Out of the small number of studies devoted to this problem let us mention pioneering work of Hampel *et al.*[6] where a layered version of the Korringa-Kohn-Rostocker (KKR) method has been used for the calculation of the local magnetic moments around the $\Sigma5(310)$ symmetrical tilt GB in iron. These authors report an enhancement of the local magnetic moment at the grain boundary, similar as at the (100) iron surfaces. The calculated value of the magnetic moment at the GB was 2.56 μ_B, the bulk value is 2.22 μ_B. Their results were obtained for a *nonrelaxed* GB and, therefore, they may be not very realistic. The same GB in iron was investigated using a Green functions approach within tight-binding linear-muffin-tin-orbital (TB LMTO) method.[7] The enhancement of the local moment was confirmed, but the local magnetic moment found at the GB was somewhat larger, even 2.74 μ_B. Wu *et al.*[8] calculated a local magnetic moment at the $\Sigma3(111)$ GB in iron and obtained the same value for unrelaxed and relaxed GBs 2.60 μ_B. There are some other recent studies of GBs in ferromagnetic iron,[9,10] but none of them analyzes the magnetic moment distribution around the GB. Only very recently, Wachowicz and Kiejna[11] analyzed local magnetic moments around the $\Sigma5(210)$ GB in iron. They obtained a similar increase of the magnetic moments at the GB and their oscillatory decay toward the bulk value as in our work.

On the other hand Szpunar *et al.*[12] studied two twist grain boundaries in nickel [$\Sigma5(100)$ and $\Sigma13(100)$] and obtained local magnetic moments at the GB about 15% smaller and almost the same compared to those in the bulk, respectively. For the structural optimization they used molecular dynamics with an embedded atom potential. Then the electronic structure was calculated with the help of the tight-binding linear-muffin-tin-orbital method within the atomic sphere approximation. A similar result concerning the $\Sigma3(11\bar{2})$ tilt grain boundary in nickel was reported by Siegel and Hamilton[13] where no difference in magnetization at the grain boundary relative to the bulk atoms was observed. This was calculated using a plane-wave basis set and ultrasoft pseudopotentials. Both these results were obtained within the local-density approximation for exchange and correlation. Geng *et al.*[14] investigated the $\Sigma5(210)$ GB in nickel using the full-potential linearized augmented plane-wave (FLAPW) method and the generalized-gradient approximation. The local magnetic moment of nickel atoms at the GB was found to be 0.67 μ_B, slightly enhanced with respect to the bulk (0.60 μ_B). Experimentally, the magnetic moment at the twist GB in nickel [twist angle in (100) plane $\phi_t=19.7°$] was determined to be more than two times higher (1.6 μ_B) than in bulk nickel.[15] Unfortunately, this GB could hardly be treated within a DFT approach because of the necessity of using a very large supercell.

All these investigations were performed for clean GBs, i.e., without segregated impurity atoms. However, it is known that the presence of impurities at GBs strongly influences many mechanical and magnetic properties. The thermodynamic model proposed by Rice and Wang[16] has been used in several studies[17–20] of GB segregation and fracture behavior within first-principles calculations. One of the most prominent (and still not resolved) problems is Bi segregation at the GBs in Cu.[21–23]

The influence of the ferromagnetic transition on the segregation of impurities has already been studied

experimentally.[24,25] It was found, for example, that in Co-50%Ni alloys the segregation of Sb and S is intensified when the transition to the magnetic state of the alloy is achieved.[25] Very recently, the application of an external magnetic field to control the segregation of impurities to the GBs was proposed.[26,27] After a so-called magnetic annealing, the concentration of Sn impurity atoms at the GBs in iron-tin alloys was found to be the same as in the bulk although before the annealing it was 1.5 times higher. These experimental findings show the importance of magnetism at the GBs.

The present work can be regarded as one of the first attempts to study magnetism of GB with segregants on the *ab initio* level. We focus on iron where the $\Sigma5(310)$ symmetrical tilt GB is considered, and on nickel where we investigate the $\Sigma5(210)$ symmetrical tilt GB. The main purpose of this work is to extend previous theoretical results for these GBs, including structural relaxation and magnetism, with the help of reliable first-principles calculations. The segregation of tin and silicon as substitutional and interstitial impurities at the GBs in iron and their influence on the electronic structure and the local magnetic moments in the vicinity of the GBs is also examined. Further, we calculate the segregation enthalpies and compare them with experiment.

The paper is organized as follows: after Introduction, Sec. II gives the details of the calculations and description of our structural model. Section III is devoted to the results for clean $\Sigma5(310)$ GB in iron and Sec. IV discusses the effect of segregants at this GB. The results for $\Sigma5(210)$ GB in nickel are contained in Sec. V. Conclusions are presented in Sec. VI.

II. COMPUTATIONAL DETAILS AND MODEL

All calculations were performed within the density-functional theory (DFT) using the Vienna Ab-initio Simulation Package (VASP) code[28–30] in which the projector augmented waves (PAW) method[31,32] is implemented. For the exchange-correlation energy, the generalized gradient approximation[33] (GGA) was employed, which is necessary to obtain a correct ground state for iron. The Brillouin zone (BZ) was sampled using the Monkhorst-Pack scheme and the BZ integration was performed either by the Methfessel-Paxton or by the tetrahedron method, depending on whether relaxations or static calculations were carried out. In a plane-wave basis the Hellman-Feynman forces acting on atoms can easily be computed. The total energy was minimized with respect to the atomic positions within the supercell. A combination of two methods of relaxation was employed, namely, the conjugate gradients method and the quasi-Newton method. The relaxation was performed as follows: first we applied the conjugate gradient method, which is robust for states far from the equilibrium. Then we continued by the quasi-Newton method, which is more efficient close to the equilibrium. The cutoff energy restricting the number of plane waves in the basis set was $E_{\mathrm{cut}}=270$ eV for both iron and nickel. In all calculations we used a $6\times2\times18$ **k**-point mesh resulting in 27 **k** points in the irreducible part of the Brillouin zone. Local and orbital-projected densities of states (DOSs) were obtained by projecting the wave functions onto spherical harmonics within spheres around each atom, the radii being equal to the Wigner-Seitz radii.

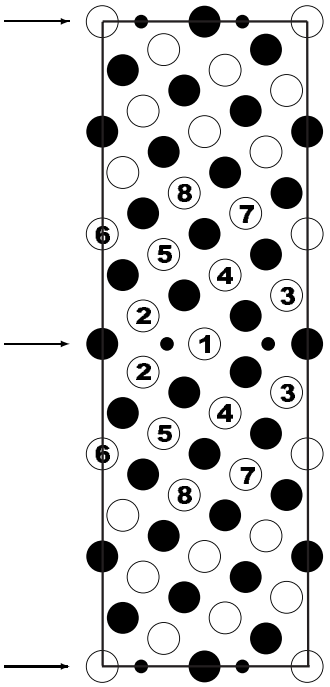

FIG. 1. The supercell used in calculations of the $\Sigma5(310)$ GB in iron viewed along the [001] direction. Full and empty circles mark the atoms in the $z=0$ and $z=a/2$ planes, respectively, a is the lattice constant. Small full circles represent positions of interstitial impurity atoms. The grain-boundary planes are indicated by arrows. Explicit numbering of atomic layers in the vicinity of the GB is given, starting from the GB plane which has number 1.

In this work we study two types of GBs, namely, $\Sigma5(310)$ in bcc iron and $\Sigma5(210)$ in fcc nickel. Here we use the well-known coincidence site lattice (CSL) notation, Σ being the inverse density of CSL sites.[34] A $\Sigma5(310)$ GB is created by rotating two bcc grains around the [001] axis by 36.9°; the (310) plane is the GB plane. To get a $\Sigma5(210)$ GB we rotate two fcc grains around the [001] axis also by 36.9°. Both GB structures are modeled by a supercell containing 60 non-equivalent atoms with two equivalent, reversely oriented grain boundaries as can be seen from Fig. 1. Every atomic layer parallel to the GB plane contributes by two atoms to the supercell. The first coordination shell of the atoms in the layer 1 (GB plane) consists of four atoms in layer 2 and four atoms in layer 3. The distance to these nearest neighbors is the same as in bulk iron, 2.46 Å.

Substitutional impurity atoms are considered to occupy the whole GB plane—layer 1 in Fig. 1. Interstitial impurity atoms are in positions which correspond to the small black circles in Fig. 1. In order to obtain the equilibrium lattice parameters, we performed for both elements a volume relaxation of the ground-state structures and found $a=2.835$ Å [the experimental value is $a=2.867$ Å (Ref. 35)] for bcc iron and $a=3.518$ Å [the experimental value amounts to $a=3.524$ Å (Ref. 36)] for fcc nickel. The dimensions of the supercells are then $8.966\times26.897\times2.835$ Å^3 for iron and $7.866\times23.599\times3.518$ Å^3 for nickel. The distance between two GB planes is 13.449 Å in case of the $\Sigma5(310)$ GB in

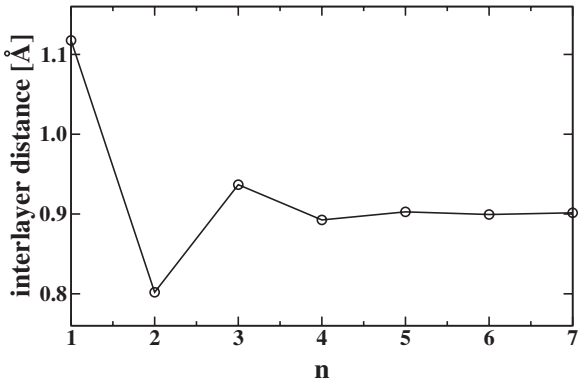

FIG. 2. Interlayer distance vs distance from the Σ5(310) GB plane in Fe in terms of numbering introduced in Fig. 1. On the horizontal axis the number n corresponds to the interlayer distance $d_{n,n+1}$ between nth and $(n+1)$th layer. The interlayer distance in bcc Fe is 0.90 Å.

iron and 11.800 Å for the nickel Σ5(210) GB. This value corresponds to 15 atomic layers. This is enough to remove any interaction of GBs with their periodic images, as it is indicated by the values of the local magnetic moments in the two central planes between the GBs (planes 8 and 9); a detailed discussion is given below. The values of local magnetic moments in these two planes are essentially the same as for bulk iron and nickel.

III. CLEAN Σ5(310) GB IN IRON

A. Structure of grain boundary

In this section we will focus on the clean Σ5(310) GB in iron. The atomic positions after the relaxation are only modestly changed compared to the original unrelaxed structure. Almost all the changes regard the atoms in the second layer. Figure 2 shows the variation of the interlayer separation with increasing distance from the GB. We see a damped oscillatory behavior. The first interlayer distance at the GB is expanded by 0.22 Å, the second contracted by 0.10 Å, and so on. From the fourth layer on, the (calculated) bulk value (0.90 Å) is essentially reproduced. This shows that the slab used in the calculations is large enough to grasp the main properties of GBs distinct from the bulklike behavior. The expansion of d_{12} is a direct consequence of the lattice mismatch at the GB, while the ocillatory variation of the further interlayer distances follows from the different response of s and d electrons to the volume expansion at the GB. The mobile s electrons around the atoms in the second layer relax into the region of reduced electron density, while the tightly-bound d electrons remain close to the ionic cores. As shown by Pettifor[37] the local internal pressure in a transition metal consists of an s electron contribution favoring expansion (as a consequence of the kinetic energy of the s electrons) and of a compressive d-electron contribution reflecting the strong d-d binding. Hence the reduced s-electron density around the second-layer atoms shifts the balance in the direction of the compressive d-electron pressure, causing a local contraction.

Similar oscillations of the atomic positions were observed in a vicinity of the metal surfaces. It was shown[38] that these are a result of the redistribution of the charge density. At the surface, the top layer relaxes inwards due to the reduced coordination of the surface atoms and the strength of the back bonds is increased (bond-order conservation). The locally increased electron density causes an expansion of the distance between the subsurface layers.

Another interesting result is the full mirror symmetry of the GB. In previous studies of the structure of a Σ5(310) GB in Mo,[39] Nb,[40] and Ta,[41] investigated by means of the model generalized pseudopotential theory (MGPT), a breaking of the mirror symmetry was found for Mo and Ta, but not for Nb. A similar result was obtained also by Ochs *et al.*[42] In MGPT, the interatomic forces are described by pair- and three-body potentials, while our *ab initio* calculations give the full account of quantum many-body forces.

B. Grain-boundary energy

The grain-boundary energy (formation energy of a GB) γ_{gb} is defined as the energy needed to create a GB in the bulk material. Within the *ab initio* approach it can be calculated as the difference of the total energies of two supercells: one with the GBs and the other one without them. The supercell of the perfect crystal has the same volume and shape as the supercell with the GBs. This difference is then divided by the area of the GBs, i.e., twice (we have two GBs within it) the cross section of the supercell. Our calculated value is $\gamma_{gb}=1.63$ J m^{-2}. Hyde *et al.*[3] obtained, using a molecular statics approach without spin polarization, a value of 1.10 J m^{-2}. Embedded atom method (EAM) calculation of Watanabe *et al.*[43] yields a GB energy of 1.30 J m^{-2}, also without magnetic effects. Yeşilleten *et al.*[44] used a semiempirical tight-binding approach, combined with a Stoner-like description of the magnetic exchange interactions and assumed a power-law relationship between the interatomic potentials and the hopping integrals to calculate the formation energies of a number of GB in iron. No information on the size of the model used to describe the GB is given. Information on the structure of the interface is restricted to the outward motion of the planes immediately at the interface which is somewhat larger (0.26 Å, i.e., nearly 30% of the bulk interlayer distance) than found in our study. Similar discrepancies exist also for the magnetic moments which are larger than our results by about 0.25–0.30 μ_B, both in the bulk and at the interface. It is therefore difficult to relate their very low value of $\gamma_{gb}=0.56$ J m^{-2} to our results.

The only experimental value we have found[45] is rather old and amounts to $\gamma_{gb}=0.77$ J m^{-2}. This number does not represent a particular value for Σ5(310) GB, but it is probably an average value for GBs typically occurring in iron. It is about two times smaller than our result. The overestimation of the GB energy may be related to two effects: (i) Density-functional calculations tend to overestimate surface energies. (ii) The size of the computationally accessible models is still rather modest. It has to be left to further studies, both experimental and theoretical, to asses the accuracy of current prediction of GB energies.

C. Magnetism at the grain boundary

We now turn to the analysis of the magnetic profile around a GB. We calculated layer-resolved values of local

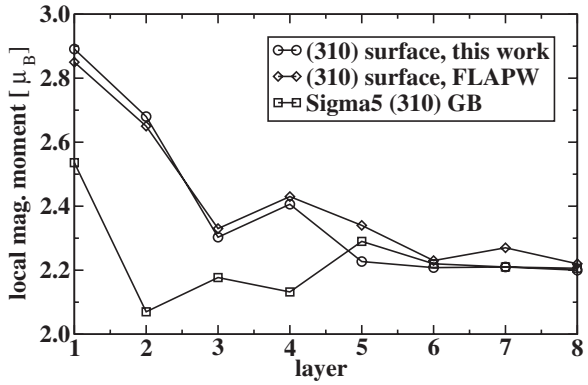

FIG. 3. Local magnetic moments of iron atoms in the neighborhood of a Σ5(310) GB. Numbering of atomic layers along the horizontal axis is the same as in Fig. 1. For comparison we also show the distribution of magnetic moments for (310) iron surface. Circles and squares mark our results, diamonds are FLAPW results (Ref. 46).

magnetic moments in the vicinity of the GB. The results are shown in Fig. 3. The values of the local magnetic moments of atoms in the neighborhood of a relaxed (310) iron surface are displayed for comparison. The most striking fact is the enhancement of the local moments of atoms in the GB plane to 2.55 μ_B. Neglecting structural relaxation, this was already highlighted by some authors,[6,7] but here we account for the full structural relaxation and confirm this fact even for a relaxed GB. It is interesting to consider the magnetic profile of *nonrelaxed* GB, see Fig. 4. Our nonrelaxed results are in very good agreement with previous calculations of Turek *et al.*[7] In both cases, we see an enhancement of local moments (2.79 μ_B and 2.75 μ_B, respectively) at the GB. From the sixth layer on, the bulk value of the magnetic moment is correctly reproduced. The largest difference from the relaxed results is that the behavior of magnetic moments is monotonic for the unrelaxed configuration, i.e., without oscillations. The earlier work of Hampel *et al.*[6] gives a qualitatively similar result, but the predicted enhancement is not as large (about 2.56 μ_B) and even at a large distance from the GB the

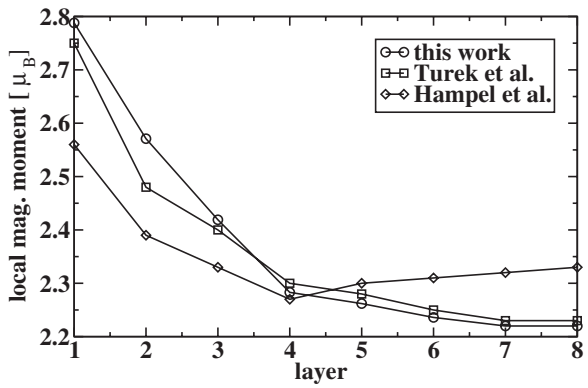

FIG. 4. Local magnetic moments of iron atoms in the neighborhood of the *nonrelaxed* Σ5(310) GB. The numbering of atomic layers along the horizontal axis is the same as in Fig. 1. The results of Turek *et al.* (Ref. 7) and of Hampel *et al.* (Ref. 6) are shown for comparison.

local magnetic moment does not approach the bulk value, being higher than 2.3 μ_B.

Comparison of Figs. 2 and 3 shows that the values of local magnetic moments essentially follow the oscillations in the interlayer spacing between layers. After the relaxation, the atoms in the GB plane have a local environment consisting of four atoms at a distance of 2.51 Å in layer 3 and four atoms at a distance of 2.54 Å in layer 2. In bulk iron atoms have eight nearest neighbors at 2.46 Å. This shows that the higher local magnetic moment of atoms in the GB is to a large extent a magnetovolume effect. To confirm this, we also calculated the local atomic volume for each atom by constructing a Voronoi[47] polyhedron around each site. The faces of this polyhedron are perpendicular bisectors of the vectors connecting an atom to its nearest neighbors. In bulk iron the calculated atomic volume is 11.39 Å^3. At the GB the atomic volume is increased to 12.59 Å^3 [see also Fig. 7(b)]. This corroborates the magnetovolume origin of the higher local moments. However, this argument cannot be applied to the more distant layers. For atoms in the second layer from the GB, the calculated Voronoi volume of 11.86 Å^3 is still larger than the atomic volume in the bulk, but the magnetic moment is reduced. The reason is that the relaxation around the second layer is strongly asymmetric. The distances to the atoms in the mirrored second layer (across the GB, 2.23 Å) and to the atoms in the third layer (2.39 Å) are smaller than in the bulk and the reduced distances cause a reduction of the magnetic moment, overriding the expansion of the distorted Voronoi polyhedron.

We expect that even in the highly distorted region around the GB the Stoner picture of the itinerant magnetism is valid for the local magnetic moments, as suggested by the work of Turek and co-workers on amorphous iron[48] and on crystalline and amorphous transition-metal alloys.[49] Motivated by experimental work of Himpsel[50] who had demonstrated an apparent universality of the ratio of the *average* exchange splitting to the average magnetic moment for a wide class of systems, ranging from the ferromagnetic elements to spin glasses, magnetic overlayers, and free atoms, Turek and co-workers[48,49] investigated the correlation between the *local* exchange splitting Δ_i and the local magnetic moments μ_i. They confirmed that the correlation is strictly linear with a slope $\Delta_i/\mu_i = I \simeq 1$ eV/μ_B. The parameter I corresponds to the Stoner exchange parameter in the theory of itinerant ferromagnetism. We find that the same correlation holds for Fe atoms in the vicinity of a grain boundary. We calculated the local exchange splitting for atoms up to eighth layer as the difference in the positions of the centers of gravity of the local DOSs for spin-up and spin-down electrons and plotted it against the local magnetic moments of corresponding atoms. The layer-resolved local DOSs are shown in Fig. 5. We see the evolution from the first layer, where spin-down bonding states below the DOS minimum are not fully occupied (leading to a higher local magnetic moment), to the third layer where the DOS is already very similar to the DOS of bulk iron. The relation of the calculated local exchange splitting to the local magnetic moment is shown in Fig. 6. We find that this relation is nearly linear and a least-squares fit gives a slope of $I = 1.01$ eV/μ_B, which is essentially identical to the experimental value of Himpsel[50] and the theoreti-

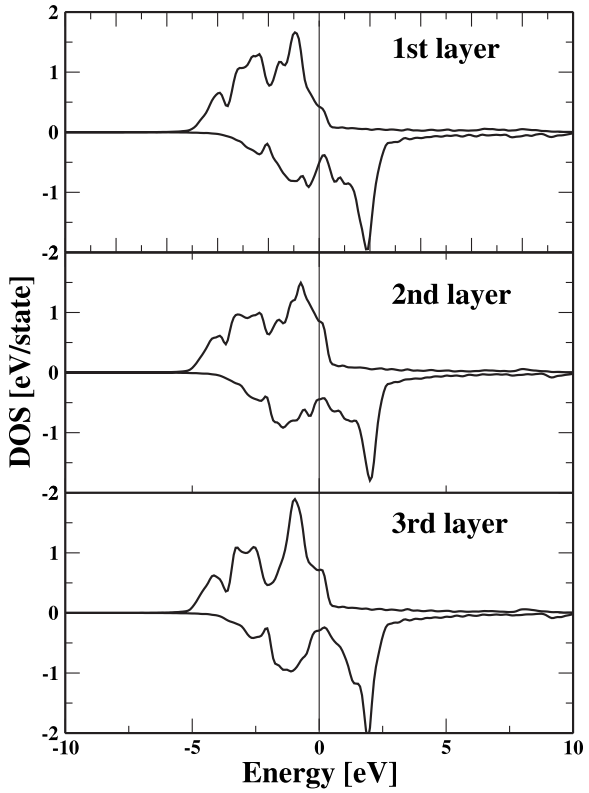

FIG. 5. Local DOS of iron atoms lying in the first three layers of the Σ5(310) GB. The Fermi energy E_F is set to zero.

cal values found by Turek and co-workers.[48,49] Our analysis demonstrates that the Stoner theory of itinerant ferromagnetism in disordered systems also describes the variation of the local magnetic moments near a GB.

In Fig. 3 we have compared the variation of the magnetic moments near a GB and near a surface—in both cases the moments are strongly enhanced, but the physical mechanisms causing the enhancement are different. At the free surface, the enhancement is caused by the reduced coordination, in spite of the inward relaxation of the surface layer. At the GB, the coordination number is the same as in the bulk, and the volume expansion drives the enhancement of the magnetic moment. A good agreement of our results with those of Geng *et al.*[14] is a further confirmation that the PAW calculations achieve the same level of accuracy as the all-electron calculations, even for transition-metal surfaces.[51]

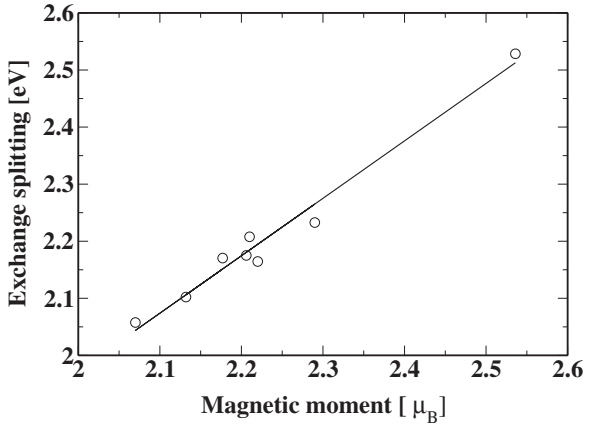

FIG. 6. Correlation of the local exchange splitting and the local magnetic moments for atoms around clean Σ5(310) GB in iron.

IV. Σ5(310) GB IN IRON WITH SEGREGANTS

In this section we study the same Σ5(310) GB in iron with segregated impurity atoms (silicon or tin). Both interstitial and substitutional impurity sites are considered.

The supercell used for the calculations with a substitutionally segregated impurity is identical to that used for clean grain boundaries, except that two atoms in both GB planes are now silicon or tin atoms. This means that the whole GB plane is occupied by impurity atoms. The interstitial impurities are considered to occupy two interstitial "holes" in both grain-boundary planes. These holes are indicated as small black circles in Fig. 1. Hence the number of atoms in the supercell is increased from 60 to 64 in the case of interstitial segregants.

A. Substitutional segregation

In Fig. 7 we display the dependence of the local magnetic moments (upper panel) and the local atomic volumes (lower panel) on the distance from the GB. For comparison, the results for a clean GB are also included. For substitutionally segregated silicon, the local environment of atoms in the GB plane is almost unchanged when compared to the clean GB. The local atomic volume of a Si atom is a little bit smaller (by 0.3 $Å^3$), the distances of nearest and next-nearest neighbors are 2.45 Å (2.51 Å for clean GB) and 2.55 Å (2.54 Å for clean GB). After relaxation the nearest neighbors of a substitutional Si atom lie in the *third*, not in the second layer, as it is the case of clean GB. This indicates that the local environment of a segregated Si atom is appreciably distorted. The strong Fe-Si interaction and the reduced site symmetry lead to a local DOS on Fe atoms in the second layer which is broadened and where the characteristic structure of the DOS of a bcc transition metal has largely been lost [see Fig. 8(c)]—both effects disfavor magnetism. The spin-up DOS is less populated (by 0.14 electron) and spin-down band is more populated (by the same amount) as compared to the clean GB. This gives rise to a smaller value of the magnetic moment (1.79 μ_B) for iron atoms in the second layer.

The same applies to the iron atoms in the third layer. We have already mentioned that these atoms are even closer to the Si atom than the atoms from the second layer, so we could expect a stronger decrease of the local magnetic moment. However, it is not so, because the iron atoms in the second layer have four silicon atoms in its neighborhood, the atoms in the third layer only two. The difference in local magnetic moments is only 0.11 μ_B; the atoms in the third layer have a magnetic moment of 1.90 μ_B, see Fig. 7(a). The values of local magnetic moments in subsequent layers exhibit oscillations around the bulk value. The substitutional Si atoms exhibit a small negative magnetic moment of −0.11 μ_B. We can compare this value with the *ab initio* calculations of Dennler and Hafner[52] on Fe_3Si who obtained the

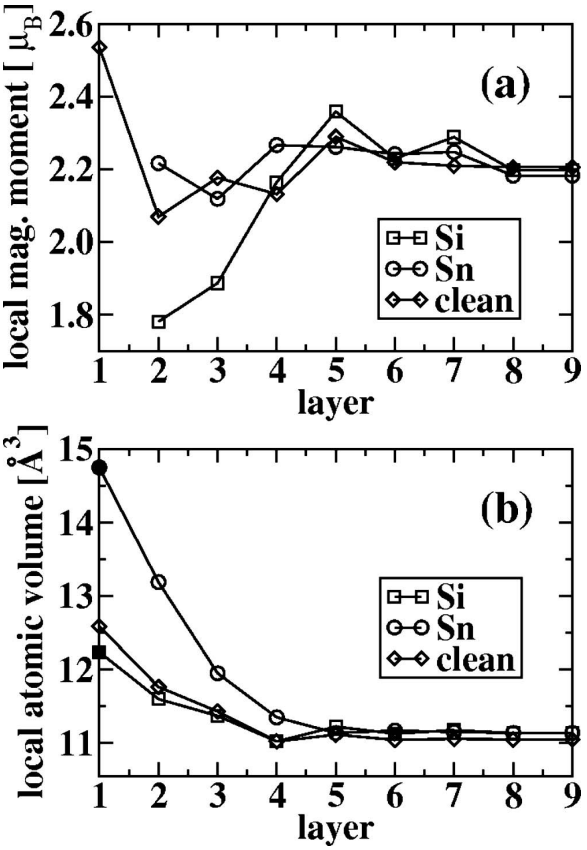

FIG. 7. The effect of substitutionally segregated silicon and tin on the local magnetic moments (a) and the local atomic volumes (b) at iron atoms from the second layer to the bulk in the Σ5(310) GB in iron. In (b), the volumes shown for the first layer correspond to segregated silicon (a full square) and tin (a full circle) in the GB plane. Let us note that here we are faced with a slight difference in the bulk atomic volumes obtained from the bcc bulk and GB supercell calculations. Due to a finite size of our model, the atomic volume in the bulklike material in the GB supercell (layers 6–9) approaches a value of 11.05 Å^3, whereas the atomic volume in the bcc bulk iron amounts to 11.39 Å^3. This difference (about 3%) does not influence the conclusions of the present work.

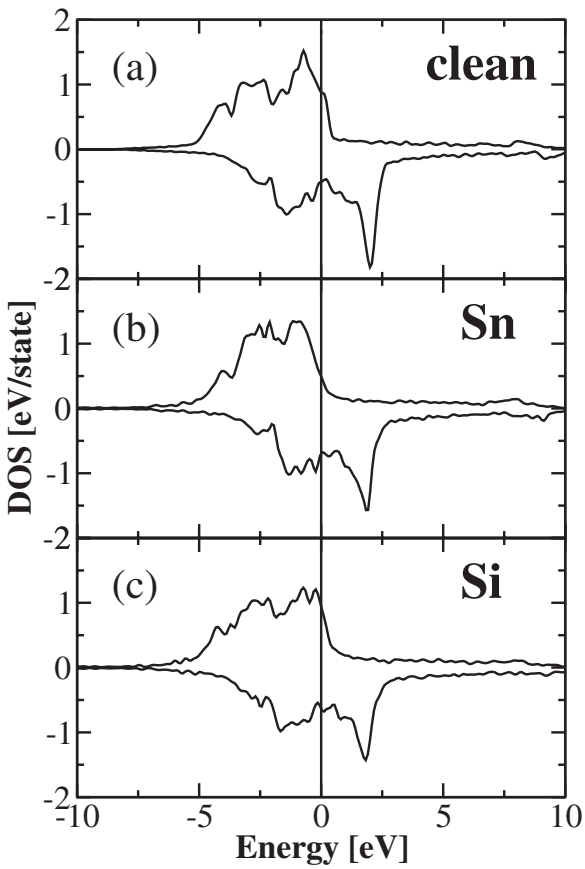

FIG. 8. Local DOS of iron atoms lying in the second layer (a) for clean Σ5(310) GB, (b) for the Sn-segregated, and (c) for the Si-segregated GB. The Fermi energy E_F is set to zero.

same value for Si atoms in $D0_3$ structure. The experimental estimation[53] is −0.07 μ_B which is in a good agreement with our value.

The magnetic profile of a Sn-decorated GB in Fig. 7(a) shows that the local magnetic moments are only very little affected, with the values oscillating close around the bulk value. The modest change of the magnetic moments compared to the clean GB is the consequence of two effects acting in opposite directions. The larger size of Sn atom causes a strong local expansion [by 1.3 Å^3 for iron atoms in the second layer, see Fig. 7(b)] and a band narrowing [see Fig. 8(b)]; the strong Fe-Sn hybridization changes the structure of the local DOS. As a result, the magnetic moments in layers adjacent to the GB are essentially unaffected. The magnetic moment of substitutional Sn atom is −0.12 μ_B.

We also investigated possible changes in the Stoner-like behavior found for the clean GB (Fig. 6) when the segregants are present. The dependence of the local exchange splitting and local magnetic moments of iron atoms follows the same linear correlation as for the clean GB. When taking into account only iron atoms lying in the first three layers and thus under the largest influence of the segregant-iron atom hybridization we obtain the value of I=0.97 eV/μ_B for segregated Si and I=0.96 eV/μ_B for Sn. This smaller local exchange splitting can be expected as the hybridization leads to the filling of the characteristic bonding-antibonding pseudogap and smearing of the peaks [see Figs. 8(b) and 8(c)].

B. Interstitial segregation

The dependence of the local magnetic moments and atomic volumes on the layer number for interstitial segregation of Si and Sn are shown in Fig. 9. Compared to substitutional impurities at the GB, the expansion of the local atomic volume and the variation of the magnetic moments extend to much larger distances from the GB. This effect is most pronounced for tin [Fig. 9(b)]. The distances between the second layers on both sides of the GB are 2.97 Å for tin and 2.87 Å for silicon (in the substitutional case, the distances are 2.20 Å for silicon and 2.51 Å for tin).

For interstitial Sn at the GB, the variation of the magnetic moments is again determined by two competing effects. Very close to the GB, the volume expansion favoring a band narrowing and an enhanced magnetic moment and the Fe-Sn hybridization disfavoring magnetism largely counterbalance

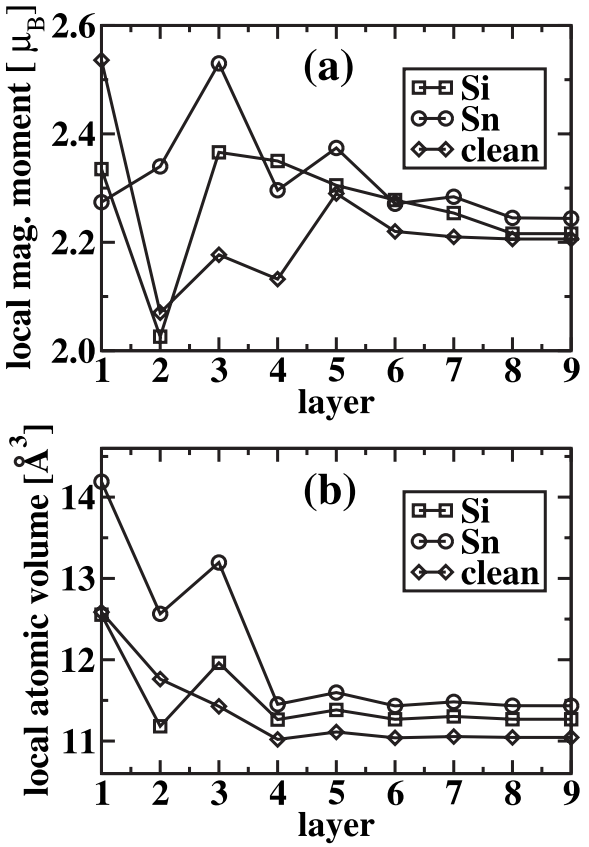

FIG. 9. (a) The effect of interstitially segregated silicon and tin on local magnetic moments and (b) on local atomic volumes at iron atoms from the second layer to the bulk in the Σ5(310) GB in iron. The magnetic moments and volumes for the first layer correspond to iron atoms in the GB plane. Due to a finite size of our model, the atomic volumes in the bulklike region (layers 6–9) approach a value slightly different from the atomic volume of the bcc bulk iron (11.39 Å^3); this small difference does not influence the conclusions drawn in the present work.

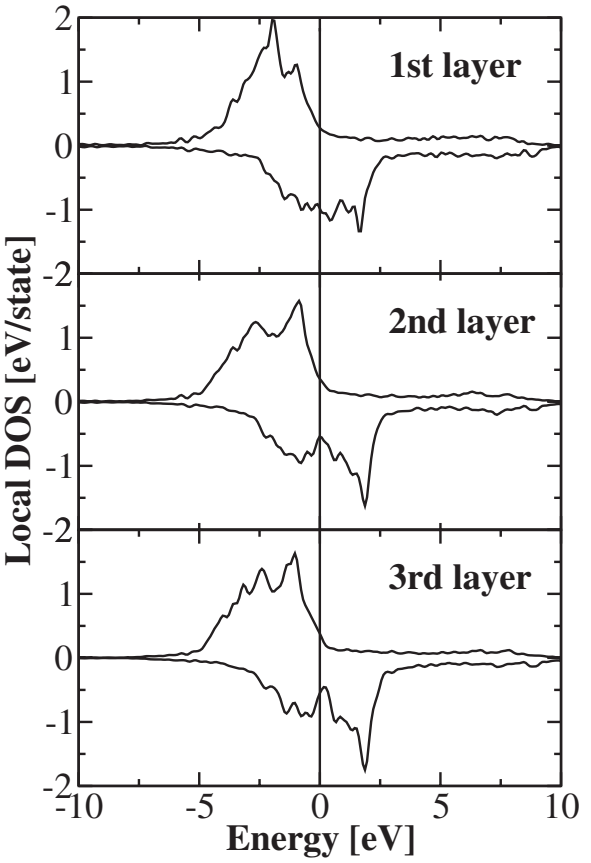

FIG. 10. Local DOS of iron atoms lying in the first three layers from the Σ5(310) GB with interstitial tin atoms. The Fermi energy E_F is set to zero.

each other. In the third layer, however, the Fe-Sn interaction is already too weak and the volume expansion causes a large enhancement of the magnetic moment. This is also reflected in the local DOS, see Fig. 10. For iron atoms in the GB layer (local volume 14.2 Å^3) both spin channels are strongly smeared, with spin-up *d* bands nearly entirely filled.

In the third layer, the local DOS for the spin-down bands already exhibits a bonding-antibonding splitting with the minimum slightly above the Fermi energy. This splitting leaves some bonding states unfilled, which results in a large value of local magnetic moment in the third layer.

The profile of local volumes and magnetic moments near a GB with interstitial Si is similar to that of a clean GB. The most evident difference is the oscillatory variation of the volume, compared to the monotonic decay for a clean GB. The larger volume in the third layer is also reflected in a locally increased magnetic moment.

C. Segregation enthalpies

The segregation enthalpy of impurities at a GB can be measured. It is defined as the lowering of the energy of the system when solute atoms go from the bulk to the GB. We calculated the segregation enthalpies for both segregation sites and both elements. In the *ab initio* calculations we obtain the segregation enthalpy as the difference of total energies of two supercells. For substitutional impurities, two atoms in the eighth layer in both grains are substituted by silicon or tin, interstitial impurities are embedded to the "holes" between eighth and ninth atomic layer. Then we subtract the total energy of this supercell from the total energy of supercell with segregants as described above. The results are summarized in Table I. Experimentally it is known[54,55] that silicon is a substitutional segregant while tin segregates to interstitial sites. Our calculations confirm this result. Note that for substitutional tin we get a positive value of segregation enthalpy signalizing the instability of that position. Experimental values of segregation enthalpies for tin[56] and silicon[57] are in reasonable agreement with our calculations, see Table I.

TABLE I. Table of segregation enthalpies of silicon and tin. The values are in kJ/mol.

	Si	Sn
Interstitial, (exp.)	−9	−19, (−22.5)
Substitutional, (exp.)	−16,(−8.5)	8

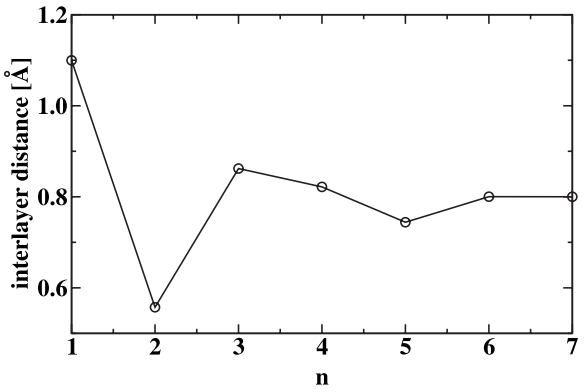

FIG. 11. Interlayer distance vs distance from the Σ5(210) GB plane in Ni in terms of numbering introduced in Fig. 1. On the horizontal axis the number n corresponds to the interlayer distance $d_{n,n+1}$ between nth and $(n+1)$th layer.

V. Σ5(210) GB IN NICKEL

For simulation of Σ5(210) GB in nickel we have used a similar model as presented in Fig. 1. The main difference is that iron has the bcc and nickel the fcc structure. However, the geometrical structure of the GB plane remains the same.

In Fig. 11, we display the interlayer distance as a function of the distance from the GB after the relaxation. The profile is similar as for a GB in iron but the oscillations are long ranged. Only at the interlayer distance d_{67}, the bulk value 0.80 Å is reached. The interlayer distance d_{12} increases by about 0.30 Å. This is larger than for iron, where an increase by about 0.22 Å was observed. In Fig. 12 we show the calculated distribution of magnetic moments around this GB and compare them with the work of Geng *et al.*[14] who used the FLAPW method. As we have seen in Fe, the local expansion at the GB leads to a considerably enhanced magnetic moment: $\mu_1=2.55\ \mu_B$ at the GB compared to $\mu_0=2.20\ \mu_B$ in the bulk; the corresponding atomic volumes are $V_1=12.59$ Å^3 and $V_0=11.39$ Å^3 (see Sec. III). In Ni, the atomic volumes in the first GB layer and in the bulk are $V_1=12.62$ Å^3 and $V_0=10.89$ Å^3, respectively; the corresponding magnetic moments are $\mu_1=0.67\ \mu_B$ and $\mu_0=0.60\ \mu_B$. Now, the question is how to compare the size of the magnetovolume effect. If we divide μ_1/μ_0 by V_1/V_0, then we obtain 1.05 for the Fe GB and 0.96 for the Ni GB, i.e., relatively, in the Fe GB the magnetic moment in the first layer increases somewhat faster than the volume and in Ni GB somewhat slower than the volume, so that according to this criterion, the magnetovolume effect at the Ni GB is a little bit weaker than at the Fe GB. If we, however, divide the difference $\mu_1-\mu_0$ by the ratio V_1/V_0, then we obtain a "normalized" change of 0.32 μ_B and 0.06 μ_B for the Fe GB and Ni GB, respectively. Thus, according to this criterion, the magnetovolume effect in Ni GB is considerably weaker than at the Fe GB. It is a little bit surprising that the magnetic moment of the atoms in the second layer is slightly higher than that of the atoms in the GB layer.

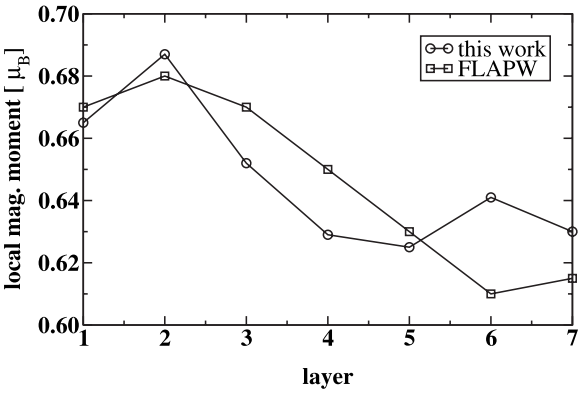

FIG. 12. Local magnetic moments of nickel atoms in the neighborhood of Σ5(210) GB. Numbering of atomic layers along the horizontal axis is the same as in Fig. 1. For comparison we also show FLAPW results[14] which are marked by squares. Our results are displayed as circles.

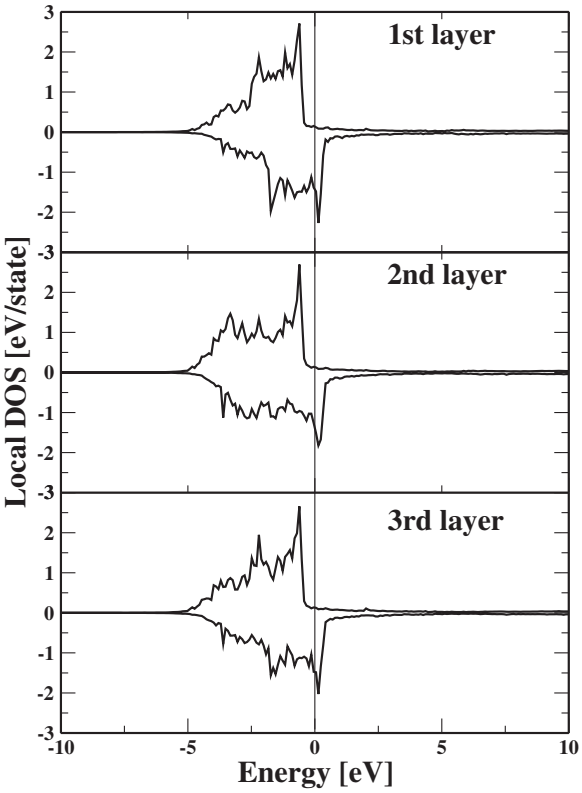

FIG. 13. Local DOS of nickel atoms lying in the first three layers from the Σ5(210) GB. The Fermi energy E_F is set to zero.

In Fig. 13 we show layer-resolved DOSs for nickel atoms around the GB from the first to the third layer. It is clear that the spin-up electronic states are fully occupied for atoms in all layers. The variation of the local magnetic moments are therefore controlled by variations in the spin-down electronic states. It can be seen that the local DOS of atoms lying in the second layer is relatively more distorted and also exhibits the least occupied spin-down states—this gives slightly higher value of the local magnetic moment. These relatively small variations in electronic structure are manifestation of the weak magnetovolume effect in nickel.

VI. CONCLUSIONS

The structural and magnetic properties of the Σ5(310) symmetrical tilt GB in iron were studied using first-

principles electronic structure calculations. Three cases were considered: (1) a clean GB, (2) a GB with substitutional segregants, and (3) a GB with interstitial segregants. We confirm the enhancement of the local magnetic moment of atoms at the clean GB plane, as calculated before for nonrelaxed structures. Here we account for the full structural relaxation for the first time and predict an enhancement of the magnetic moments in the GB plane to 2.55 μ_B, i.e., by 0.35 μ_B higher than in the bulk. It is argued that this enhancement is due to a local magnetovolume effect. At larger distances from the GB the variation of the local magnetic moments follows the changes in the exchange splitting in the spin-polarized local DOS, as expected from the Stoner model of itinerant ferromagnetism.

When substitutional silicon atoms are present, the local magnetic moments of iron atoms in two adjacent layers are reduced to 1.79 μ_B and 1.90 μ_B due to the hybridization of the electronic states of silicon and iron. On the other hand substitutional tin leaves the magnetic moments unchanged because of compensation effect of volume. Interstitially segregated silicon atoms affect only the magnetic moments of iron atoms in the second layer due to their small distance after the relaxation. Finally, when interstitial tin is present at the GB, a large value of 2.55 μ_B (the same as in the clean GB plane) is found at atoms in the third layer. This effect is due to unoccupied bonding states in a spin-down channel of the local DOS. A comparison of the segregation energies shows that substitutional segregation is preferred for Si, while interstitial segregation is predicted for Sn, in both cases in agreement with experiment. At the $\Sigma 5(210)$ symmetrical tilt GB in nickel the enhancement of the magnetic moments is also predicted, but strikingly, the highest value 0.69 μ_B is found for the atoms in the second layer, *not* in the GB plane. Finally, the magnetovolume effect is found to be weaker at the Ni GB than at the Fe GB.

ACKNOWLEDGMENTS

We acknowledge the financial support from the Grant Agency of the Czech Republic (Projects No. 202/06/1509 and No. 106/05/H008), Grant Agency of the Academy of Sciences of the Czech Republic (Project No. IAA1041302) and research programs Contracts No. AV0Z20410507 (Academy of Sciences of the Czech Republic) and No. MSM0021622410 (Ministry of Education of the Czech Republic). One of the authors (M.Č.) acknowledges the support from the Marie Curie Training Site Grant and valuable help of J. Kuriplach in early stages of the calculations. The calculations were performed using the facilities of Vienna University.

[1] S. Crampin, D. D. Vvedensky, J. M. MacLaren, and M. E. Eberhart, Phys. Rev. B **40**, 3413 (1989).
[2] L. G. Wang and C. Y. Wang, Comput. Mater. Sci. **11**, 261 (1998).
[3] B. Hyde, D. Farkas, and M. J. Caturla, Philos. Mag. **85**, 3795 (2005).
[4] P. Rez and J. R. Alvarez, Acta Mater. **47**, 4069 (1999).
[5] M. Yamaguchi, M. Shiga, and H. Kaburaki, J. Phys.: Condens. Matter **16**, 3933 (2004).
[6] K. Hampel, D. D. Vvedensky, and S. Crampin, Phys. Rev. B **47**, 4810 (1993).
[7] I. Turek, V. Drchal, J. Kudrnovský, M. Šob, and P. Weinberger, *Electronic Structure of Disordered Alloys, Surfaces and Interfaces* (Kluwer, Boston, 1997), pp. 244–246.
[8] R. Wu, A. J. Freeman, and G. B. Olson, Phys. Rev. B **53**, 7504 (1996).
[9] M. Yamaguchi, Y. Nishiyama, and H. Kaburaki, Phys. Rev. B **76**, 035418 (2007).
[10] J. S. Braithwaite and P. Rez, Acta Mater. **53**, 2715 (2005).
[11] E. Wachowicz and A. Kiejna, Comput. Mater. Sci. (to be published).
[12] B. Szpunar, U. Erb, G. Palumbo, K. T. Aust, and L. J. Lewis, Phys. Rev. B **53**, 5547 (1996).
[13] D. J. Siegel and J. C. Hamilton, Acta Mater. **53**, 87 (2005).
[14] W. T. Geng, A. J. Freeman, R. Wu, C. B. Geller, and J. E. Raynolds, Phys. Rev. B **60**, 7149 (1999).
[15] M. R. Fitzsimmons, A. Röll, E. Burkel, K. E. Sickafus, M. A. Nastasi, G. S. Smith, and R. Pynn, Nanostruct. Mater. **6**, 539 (1995).
[16] J. Rice and J. S. Wang, Mater. Sci. Eng., A **107**, 23 (1989).
[17] R. Q. Wu, A. J. Freeman, and G. B. Olson, J. Mater. Res. **7**, 2433 (1992).
[18] R. Q. Wu, A. J. Freeman, and G. B. Olson, Phys. Rev. B **47**, 6855 (1993).
[19] R. Q. Wu, A. J. Freeman, and G. B. Olson, Phys. Rev. B **50**, 75 (1994).
[20] R. Q. Wu, A. J. Freeman, and G. B. Olson, Science **265**, 376 (1994).
[21] R. Schweinfest, A. T. Paxton, and M. W. Finnis, Nature (London) **432**, 1008 (2004).
[22] A. Y. Lozovoi, A. T. Paxton, and M. W. Finnis, Phys. Rev. B **74**, 155416 (2006).
[23] G. Duscher, M. F. Chisholm, U. Alber, and M. Rühle, Nat. Mater. **3**, 621 (2004).
[24] K. E. Szklarz and M. L. Wayman, Acta Metall. **29**, 341 (1981).
[25] K. Ishida, S. Yokoyama, and T. Nishizawa, Acta Metall. **33**, 255 (1985).
[26] S. Tsurekawa, K. Kawahara, K. Okamoto, T. Watanabe, and R. Faulkner, Mater. Sci. Eng., A **387-389**, 442 (2004).
[27] T. Watanabe, S. Tsurekawa, X. Zhao, and L. Zuo, Scr. Mater. **54**, 969 (2006).
[28] G. Kresse and J. Hafner, Phys. Rev. B **47**, 558 (1993).
[29] G. Kresse and J. Furthmüller, Phys. Rev. B **54**, 11169 (1996).
[30] G. Kresse and J. Furthmüller, Comput. Mater. Sci. **6**, 15 (1996).
[31] P. E. Blöchl, Phys. Rev. B **50**, 17953 (1994).
[32] G. Kresse and D. Joubert, Phys. Rev. B **59**, 1758 (1999).
[33] J. P. Perdew, K. Burke, and M. Ernzerhof, Phys. Rev. Lett. **77**, 3865 (1996).
[34] A. P. Sutton and R. W. Ballufi, *Interfaces in Crystalline Materials* (Clarendon, Oxford, 1995).

[35] R. Kohlhaas, P. Donner, and N. Schmitz-Pranghe, Z. Angew. Phys. **23**, 245 (1967).
[36] A. Taylor, J. Inst. Met. **77**, 585 (1950).
[37] D. G. Pettifor, *Physical Metallurgy* (Elsevier, Amsterdam, 1983), p. 73.
[38] J.-H. Cho, Ismail, Z. Y. Zhang, and E. W. Plummer, Phys. Rev. B **59**, 1677 (1999).
[39] G. H. Campbell, J. Belak, and J. A. Moriarty, Acta Mater. **47**, 3977 (1999).
[40] G. H. Campbell, S. M. Foiles, P. Gumbsch, M. Rühle, and W. E. King, Phys. Rev. Lett. **70**, 449 (1993).
[41] G. H. Campbell, J. Belak, and J. A. Moriarty, Scr. Mater. **43**, 659 (2000).
[42] T. Ochs, C. Elsässer, M. Mrovec, V. Vitek, J. Belak, and J. A. Moriarty, Philos. Mag. A **80**, 2405 (2000).
[43] R. Watanabe, A. Nogami, and T. Matsumyia, Mater. Sci. Forum **204-206**, 337 (1996).
[44] D. Yeşilleten, M. Nastar, T. A. Arias, A. T. Paxton, and S. Yip, Phys. Rev. Lett. **81**, 2998 (1998).
[45] L. H. Van Vlack, Trans. Am. Inst. Min., Metall. Pet. Eng. **191**, 251 (1951).
[46] W. T. Geng, M. Kim, and A. J. Freeman, Phys. Rev. B **63**, 245401 (2001).
[47] G. Voronoi, J. Reine Angew. Math. **133**, 97 (1907).
[48] I. Turek and J. Hafner, Phys. Rev. B **46**, 247 (1992).
[49] I. Turek, C. Becker, and J. Hafner, J. Phys.: Condens. Matter **4**, 7257 (1992).
[50] F. J. Himpsel, Phys. Rev. Lett. **67**, 2363 (1991).
[51] G. Kresse, W. Bergermayer, and R. Podloucky, Phys. Rev. B **66**, 146401 (2002).
[52] S. Dennler and J. Hafner, Phys. Rev. B **73**, 174303 (2006).
[53] V. A. Niculescu, T. J. Burch, and J. I. Budnick, J. Magn. Magn. Mater. **39**, 223 (1983).
[54] P. Lejček, J. Alloys Compd. **378**, 85 (2004).
[55] P. Lejček, S. Hofmann, and J. Janovec, Mater. Sci. Eng., A **462**, 76 (2007).
[56] H. J. Grabke, *Chemistry and Physics of Fracture* (Nijhoff, Dordrecht, 1987), p. 388.
[57] P. Lejček and S. Hofmann, Acta Metall. Mater. **39**, 2469 (1991).